



Research article

Contrasting Photo-physiological Responses of the Haptophyte *Phaeocystis Antarctica* and the Diatom *Pseudonitzschia* sp. in the Ross Sea (Antarctica)

Sasha Tozzi and Walker O. Smith *

Virginia Institute of Marine Science, College of William & Mary, Gloucester Pt., VA 23062 USA

*** Correspondence:** Email: wos@vims.edu

Abstract: The Antarctic is a unique environment in which substantial variations in irradiance occur over a number of time scales, and as a result phytoplankton need to acclimate and adapt to these changes. We conducted field and laboratory manipulations in the Ross Sea, Antarctica to examine photophysiological differences between *Phaeocystis antarctica* and *Pseudonitzschia* sp. a diatom that commonly occurs in the Ross Sea, since these are the two functional groups that dominate abundance and productivity. Both exhibited reduced quantum yields due to high irradiances. *P. antarctica*, a haptophyte, displays a distinct photophysiological response to irradiance when compared to diatoms. *P. antarctica* showed a rapid recovery from high light exposure, as indicated by the rapid return to initial, high quantum yields, in contrast to diatoms, which responded more slowly. Absorption cross sections were high in both forms, but those in *P. antarctica* were significantly higher. Both organisms recovered within 24 h to initial quantum yields, suggesting that high irradiance exposure does not have a permanent effect on these organisms. Among all micronutrient additions (iron, cobalt, zinc and vitamin B₁₂), only iron additions resulted in rapid impacts on quantum yields. Iron limitation also can result in reduced photosynthetic efficiency. Understanding these photophysiological responses and the impact of oceanographic conditions provides constraints on modeling efforts of photosynthesis and primary productivity in the Antarctic.

Key words: Antarctic; diatoms; photophysiology; irradiance; *Phaeocystis*; trace metals; iron

1. Introduction

Antarctic phytoplankton experience large variations in irradiance on many scales, particularly in coastal regions in the far south. The largest is seasonal, when daily solar radiation ranges to zero in winter to daily summer fluxes that exceed those in tropical areas [1]. Variations on a daily basis can be large, but are compounded by vertical positional changes within the water column generated by wind-induced mixing. Deep vertical mixing greatly reduces the irradiance available for photosynthesis by increasing the mean depth of a population, and because seawater attenuates light exponentially, mixing has a major impact on the photosynthetically active radiation available for photosynthesis. Recent advances in ocean sampling have shown that mixing varies greatly on relatively small scales (e.g., on the order of one km or less, and within a few hours) [2], which can have a significant influence on irradiance and photosynthesis. Given the extremely large variations in irradiance over different time scales, it is essential to understand the photophysiological responses of phytoplankton relative to these variations to effectively model and predict photosynthesis and productivity on all time scales.

The Ross Sea is characterized by regular occurrences of phytoplankton blooms during the austral spring and summer [3–5], with peaks of biomass and productivity observed in mid- to late December. Two functional groups, diatoms and the polymorphic haptophyte *Phaeocystis antarctica*, regularly occur [6]. *P. antarctica* has a complex life cycle [7] that includes solitary cells and colonies, the latter which often dominate blooms. *P. antarctica* blooms in early spring [8] in waters with relatively deep mixed layers [5,9], whereas diatoms are dominate in summer and occur in more strongly stratified water columns with shallow mixed layers [5]. Diatom blooms are often dominated by *Fragilariaopsis curta* [3], with *F. cylindrus*, *Chaetoceros* spp. [10], *Nitzschia* and *Pseudo-nitzschia* spp. [11] and *Thalassiosira* spp. [12] also commonly encountered. Phytoplankton distribution appears to be largely controlled by irradiance [8] and iron concentrations [13].

Photosynthetically active radiation (PAR, 400–700 nm) in the Ross Sea and its availability to phytoplankton is controlled by seasonal variations in solar elevation and inclination, ice concentration, cloudiness, and the depth of the mixed layer. Changes in these forcing factors on several different spatial and temporal scale can induce a variety of photophysiological responses such as: (a) *photoacclimation*, defined as a phenotypic response to a change in irradiance that often leads to rearrangements in the photosynthetic apparatus and changes in the photosynthetic kinetics, (b) *photoadaptation*, defined as population adjustments to changes in light regimes that occurs over a longer time scale and can involve several generations, and (c) *photoinhibition*, referred to as a combination of several different processes that result in the decline of PSII efficiency, usually as a result of high light exposure [14]. Photoinhibition usually involves fast degradation of photosynthetic

proteins following oxidative damage due to slow tyrosine electron donor activity [15]. Alternatively, photoinhibition can be caused, or exacerbated, by reduced electron flow between quinones, resulting in a slower electron turnover and increased probability of charge recombination between the primary radical pair P680 and the primary acceptor pheophytin. This event produces triplet chlorophyll that reacts with O₂ to produce extremely reactive singlet oxygen [16]. Either way, photoinhibition results in the inactivation of PSII and reduction in the pool of active PSII reaction centers. If this process becomes irreversible, or if the rates of repair lag the rates of photoinhibition, the organism will be photodamaged. There are several mechanisms of photoprotection by which organisms prevent photosynthetic apparatus damage (e.g., by reducing the rates of excitation delivery to PSII reaction center, and/or dissipating the excess of excitation energy via non-photochemical quenching). The majority of non-photochemical quenching is believed to occur through heat dissipation via the xanthophyll cycle [17].

Photophysiological responses in the Ross Sea are only partially known. Smith and Donaldson [18] used short-term ¹⁴C-uptake measurements to assess how photosynthetic rates (including light-limited and light-saturated responses) vary as a function of irradiance, season, temperature, iron concentrations, and phytoplankton composition. They found significant effects of irradiance and iron, but none attributable to composition or temperature. Arrigo et al. [19] conducted culture experiments at relatively low irradiance levels (all < 125 $\mu\text{mol quanta m}^{-2} \text{ s}^{-1}$) and concluded that a combination of pigment per cell concentrations, protective pigment production, ability to withstand photoinhibition, and excess photosynthetic capacity allowed *P. antarctica* to grow in deeply mixed, low-light environments. However, no experiments have investigated the in situ responses of Ross Sea phytoplankton on various time scales, particularly those relevant to vertical mixing. This study examined some of the photochemical responses in two forms of Ross Sea phytoplankton (haptophytes and diatoms) using variable fluorescence techniques to understand how light affects photosynthetic quantum yields and absorption cross sections of PSII. Additionally, we investigated the role of trace elements on quantum yields of natural phytoplankton assemblages.

2. Material and Methods

All experiments were conducted on the *RVIB N.B. Palmer* as part of the “Controls on Ross Sea Algal Community Structure (CORSACS)” program during cruises NBP06-01 (Dec. 2005 – Jan. 2006) and NBP06-08 (November – December 2006). Samples were collected in the southern Ross Sea [20], a region characterized by spring blooms of colonial *Phaeocystis antarctica* and summer blooms of diatoms [8]. Hence our spring cruise (NBP06-08) largely sampled *P. antarctica* assemblages, and the summer cruise (NBP-6-01) sampled diatoms. All oceanographic data are available at <http://www.bco-dmo.org/project/2072>.

2.1. Variable Fluorescence Measurements

Photosynthetic parameters based on chlorophyll a variable fluorescence were characterized using a Kolber bench-top fast repetition rate fluorometer (FRRF; [20]). This instrument is equipped with an array of blue LED lights (~470 nm) with a total power of about six watts cm^{-2} . In continuous wave mode the instrument can deliver up to 8000 μmol photons $\text{m}^{-2} \text{ s}^{-1}$ while performing FRR excitation. The FRR excitation flashlets are produced at a pulse photon flux density of about 65,000 μmol photons $\text{m}^{-2} \text{ s}^{-1}$, with 150 ns rise time and 200 ns fall time. A thermo-electric cooled 10-mm avalanche photodiode (Advance Photonics, Inc) detector is connected to an elbow-shaped light pipe that collects the emission light from the sample chamber. The instrument has a sensitivity of 0.01 $\mu\text{g chl L}^{-1}$ with 5% accuracy. The measurement protocol was optimized to obtain fluorescence saturation (F_m) by a rapid sequence of 80 flashlets, followed by 30 flashlets for the relaxation portion. Instrument blanks were determined with distilled water to assess light scattering within the cuvette, as well as seawater that had been filtered through a Millex AA 0.8 μm Millipore membrane to account for fluorescence of dissolved organic matter. All blanks were less than 1% of the maximum value[20]. The maximum quantum yield efficiency for PSII (F_v/F_m) was calculated [21] by normalizing F_m by the difference between the fluorescence at saturation (F_m) and the minimum fluorescence (F_o):

$$\Phi_{PSII}^{\max} = \frac{F_m - F_o}{F_m} = \frac{F_v}{F_m} \quad (\text{Eq. 1})$$

Functional absorption cross sections (σ_{PSII}) were calculated by fitting the fluorescence transients to a theoretical function describing the relationship between fluorescence and photosynthesis [22].

Two different units of the instrument were used. They differed only in the LED array sizes and in the signal attenuation method, but provided similar performance. Samples were either placed into the cuvette via pipette or dispensed with a peristaltic pump (maximum flow rate was 5 mL min^{-1}). To minimize condensation on the exterior of the cuvette, the light and cuvette chamber were constantly flushed with dry nitrogen gas.

2.2. Phytoplankton Cultures and Natural Assemblages

Monoclonal, non-axenic cultures of *P. antarctica* (CCMP 1374) and *Pseudonitzschia* sp. (CCMP 1445) were obtained from the Pravasoli-Guillard National Center for Culture of Marine Phytoplankton. Stock cultures were kept in duplicate 15 mL Falcon Tubes in growth chambers at $-1 \text{ }^{\circ}\text{C} \pm 1$ in filter-sterilized *f/2* media [23] under continuous irradiance (cold-white fluorescent lamps). Ross Sea phytoplankton assemblages were used for experiments shortly after collection, following removal of zooplankton by prescreening with a 200 μm Nitex mesh. Prior to measurements, the natural samples were kept under the same conditions described above. Both cultures and natural assemblages of *P. antarctica* were dominated by colonial forms.

2.3. Photorecovery (PR) Experiments

A total of five experiments were performed during the summer cruise NBP06-01, and five additional experiments were completed during the cruise (Table 1). For PR 1 *P. antarctica* and *Pseudonitzschia* sp. were kept in 1-L Qorpak bottles and acclimated to 150 $\mu\text{mol photons m}^{-2} \text{ s}^{-1}$ for 2 weeks. The F_v/F_m values of the cultures were measured at 0, 5, 10, 20 and 45 minutes after removal from the incubator while maintained on ice at $<10 \mu\text{mol photons m}^{-2} \text{ s}^{-1}$. For PR 2 a *P. antarctica*-dominated assemblage and a culture of *Pseudonitzschia* sp. were acclimated to 300 $\mu\text{mol photons m}^{-2} \text{ s}^{-1}$ for three days, and following acclimation the cultures were kept under low light ($<10 \mu\text{mol photons m}^{-2} \text{ s}^{-1}$) for two hours, and then wrapped in aluminum foil to simulate complete darkness and returned to the incubator. The cultures were sampled six times during the first hour by removing of 15 mL subsamples to determinate the rapid photorecovery kinetics, six more times in the following 12 hours, and once every 24 hours for the following 12 days to quantify the slow photorecovery kinetics. PR3 and PR4 were performed over 32 and 24 hours, respectively. Both cultures were acclimated in on-deck incubators at 50% surface irradiance for 48 h (providing an average irradiance of $\sim 400 \mu\text{mol photons m}^{-2} \text{ s}^{-1}$), after which the photorecovery was measured. PR 5 lasted 24 h and was designed to determine the effects of different exposures to inhibiting irradiance levels on photorecovery. Eight 500 mL flasks, each with 250 mL of sterile Ross Sea water, were inoculated with 50 mL of either *P. antarctica*-dominated natural assemblage or *Pseudonitzschia* sp. (4 of each). Flasks were exposed to 850 $\mu\text{mol photons m}^{-2} \text{ s}^{-1}$ for 2, 4, 6 or 8 h. During the spring cruise all experiments were conducted in indoor incubators due to the difficulty of keeping cultures from freezing in the deck incubators. PR 6, 7, 8 were performed with *P. antarctica* and *Pseudonitzschia* sp. cultures to assess photoinhibition and recovery at different irradiances. The three experiments used irradiance levels and durations of 300, 600, and 600 $\mu\text{mol photons m}^{-2} \text{ s}^{-1}$ and 3, 2 and 4 h, respectively. Photorecovery was monitored for six h after removal from light. Dominance was based on microscopic observations at sea and confirmed using chemical taxonomy after the cruise [20]. During the spring cruise *P. antarctica* on average contributed 84.5% of the total chlorophyll; during the summer cruise, diatoms contributed a smaller amount (average 41.4% of total chlorophyll) but up to 87.6% [20]. Cell concentrations of both *P. antarctica* and *Pseudonitzschia* were similar to bloom concentrations encountered in situ.

Table 1. Summary of experimental conditions used in the incubations.

Experiment ID	Phytoplankton Composition	Irradiance ($\mu\text{mol photons m}^{-2} \text{s}^{-1}$)	Temperature (°C)	Experimental Treatment
PR 1	<i>P. antarctica</i> and <i>Pseudo-nitzschia</i> cultures	150	-1.0	Incubated in constant light, then transferred to darkness to assess recovery
PR 2	<i>P. antarctica</i> and <i>Pseudo-nitzschia</i> cultures	300	-1.0	Incubated in constant light, then transferred to darkness to assess recovery
PR 3	<i>P. antarctica</i> -dominated natural assemblage and <i>Pseudo-nitzschia</i> culture	50% surface irradiance (~450)	0.0*	Incubated on deck for 48 h, then transferred to darkness to assess short-term recovery
PR 4	<i>P. antarctica</i> -dominated natural assemblage and <i>Pseudo-nitzschia</i> culture	50% surface irradiance (~450)	0.0*	Incubated on deck for 48 h, then transferred to darkness to assess short-term recovery
PR 5	<i>P. antarctica</i> -dominated natural assemblage and <i>Pseudo-nitzschia</i> culture	850	-1.0	Incubated in constant light for different intervals, then transferred to darkness to assess recovery
PR 7	<i>P. antarctica</i> and <i>Pseudo-nitzschia</i> cultures	600	-1.0	Incubated in constant light for different intervals, then transferred to darkness to assess recovery
PR 8	<i>P. antarctica</i> and <i>Pseudo-nitzschia</i> cultures	600	-1.0	Incubated in constant light for different intervals, then transferred to darkness to assess recovery
TM 1	<i>P. antarctica</i> -dominated natural assemblage	150	+1.0	Incubated in constant light to test effect of trace metal additions
TM 2	<i>P. antarctica</i> -dominated natural assemblage	150	+1.0	Incubated in constant light to test effect of trace metal additions
TM 3	<i>P. antarctica</i> -dominated natural assemblage	20% surface irradiance (~180)	+1.0*	Incubated on deck to test effect of trace metal additions

*: Mean temperature over experiment

A recovery index (REC_{ind}) was calculated as the difference in the photorecovery by comparing equal sections of the slopes of the fitted curve:

$$REC_{ind} = \frac{F_v}{F_m}_{|_{t+1}} - \frac{F_v}{F_m}_{|_t} \quad (\text{Eq. 2})$$

This approach differs from the recovery assessment calculated either as the relative recovery percentage [RR(%)] based on the maximum measured quantum yield

$$RR(\%) = 100 \frac{\frac{F_v}{F_m}_{|_i} - \frac{F_v}{F_m}_{|_{init}}}{\frac{F_v}{F_m}_{|_{max}} - \frac{F_v}{F_m}_{|_{init}}} \quad (\text{Eq. 3})$$

or as the per cent recovery based on the maximum theoretical (F_v/F_m) of 0.65 (theoretical recovery, or TR(%)):

$$TR(\%) = 100 \frac{\frac{F_v}{F_m}_{|_i} - \frac{F_v}{F_m}_{|_{init}}}{0.65 - \frac{F_v}{F_m}_{|_{init}}} \quad (\text{Eq. 4})$$

In some of the experiments, the cultures achieved complete photorecovery and maximum photosynthetic quantum yields of 0.65, so that RR approached TR.

2.4. Trace Metal Addition Experiments

Three experiments during NBP06-08 were performed to investigate the effects of trace metals and vitamin B₁₂ on phytoplankton photophysiological responses. Water was collected from 5-8 m with a trace-metal clean pump system and placed into a 50-L carboy [24], and then transferred to 2- and 4.5-L polycarbonate bottles. All water transfers were done in a positive pressure, trace metal-clean laboratory equipped with a laminar flow hood. Ambient temperature during deck incubations was maintained by a constant flow of surface seawater through the incubators. Trace additions of iron, vitamin B₁₂, cobalt, zinc were used, either singly or as additions of two trace elemental components. One nM iron was added as FeCl₃ (Fluka) in pH 2 (SeaStar HCl) MilliQ water; concentrations of added vitamin B₁₂, cobalt and zinc were 100 pM, 1 nM and 0.5 nM. All treatments were run in triplicate at 0 ± 1 °C. Trace metal concentrations were representative of pre-bloom conditions and greater than those considered to be limiting in the Southern Ocean. The first two experiments (TM 1 and 2) were performed in an environmental chamber with a constant irradiance of 150 μmol photons m⁻² s⁻¹, while the third experiment (TM 3) was performed in an on-deck incubator shielded with neutral density screen that transmitted 20% of ambient irradiance (hence providing on average ca. 160 μmol photons m⁻² s⁻¹). Samples for FRRF measurements were dark adapted in a cooler on ice for 30 to 40 minutes before measuring the maximum potential photosynthetic quantum yields and absorption cross sections.

2.5. Statistical Analysis

Photorecovery kinetics were analyzed by comparing slopes and intercepts of Ln:Ln regressions in SAS[®] using general linear model (GLM) and repeated measurements ANOVA. Comparisons between treatments were analyzed by repeated measurements ANOVA and Least Squares Means analysis with Tukey-Kramer adjustment for multiple comparisons.

3. Results

3.1. Photorecovery Experiments

In PR1 the cultures when acclimated to 150 μmol photons $\text{m}^{-2} \text{ s}^{-1}$ did not show any sign of irradiance-induced stress or photoinhibition. The initial F_v/F_m value in the *P. antarctica* culture was 0.581 (± 0.001), and the average F_v/F_m for the first 45 minutes was 0.579 (± 0.017). *Pseudonitzschia* had a slightly lower initial F_v/F_m value (0.540 ± 0.002) which remained unchanged over the next hour. In PR 2, a test of long-term photorecovery responses, cultures were acclimated to 300 μmol photons $\text{m}^{-2} \text{ s}^{-1}$, and mild photoinhibition in both the *P. antarctica*- and *Pseudo-nitzschia* cultures was observed, with initial F_v/F_m values of 0.47 and 0.48 (81 and 89% of the initial values), respectively. Their photorecovery kinetics, however, were quite different. *Pseudonitzschia* (Figure. 1) recovered slowly and showed only 30% photorecovery after 2 h, whereas 30% recovery in *P. antarctica* took only 30 minutes. After 6 and 48 h, *Pseudo-nitzschia* recovery was 50 and 99% complete, whereas *P. antarctica* recovered 70 and 94% of the maximum quantum yield over the same periods (Table 2). Slightly reduced quantum yields near the end of the experiment may represent limitation by nutrients. Photorecovery curves were significantly different ($T = -3.97$, $p = 0.0003$).

Table 2. Relative recovery (RR) percentages for the photorecovery experiments.

Experiment	Phytoplankton	Time	RR
ID	Composition	(h)	(%)
PR 1	<i>P. antarctica</i>	1	100
	<i>Pseudo-nitzschia</i>	1	100
PR 2	<i>P. antarctica</i>	1	45
		2	53
PR 2		24	93
	<i>Pseudo-nitzschia</i>	1	4
PR 3	<i>P. antarctica</i>	2	27
		24	82
PR 3	<i>P. antarctica</i>	1	39
		2	48
PR 3		8	78
		26	100
PR 3	<i>Pseudo-nitzschia</i>	1	9
		2	21
PR 3		8	60
		26	100
PR 4	<i>P. antarctica</i>	1	54
		8	100
PR 4	<i>Pseudo-nitzschia</i>	1	28
		8	89
PR 5	<i>P. antarctica</i>	6	77
		24	93
PR 5		96	96
	<i>Pseudo-nitzschia</i>	6	74
PR 5		24	68
		96	87
PR 7	<i>P. antarctica</i>	0.5	80
		1	85
PR 7		4	100
	<i>Pseudo-nitzschia</i>	0.5	87
PR 7		1	87
		8	95
PR 8	<i>P. antarctica</i>	1	25
		4	33
PR 8	<i>Pseudo-nitzschia</i>	1	14
		4	18

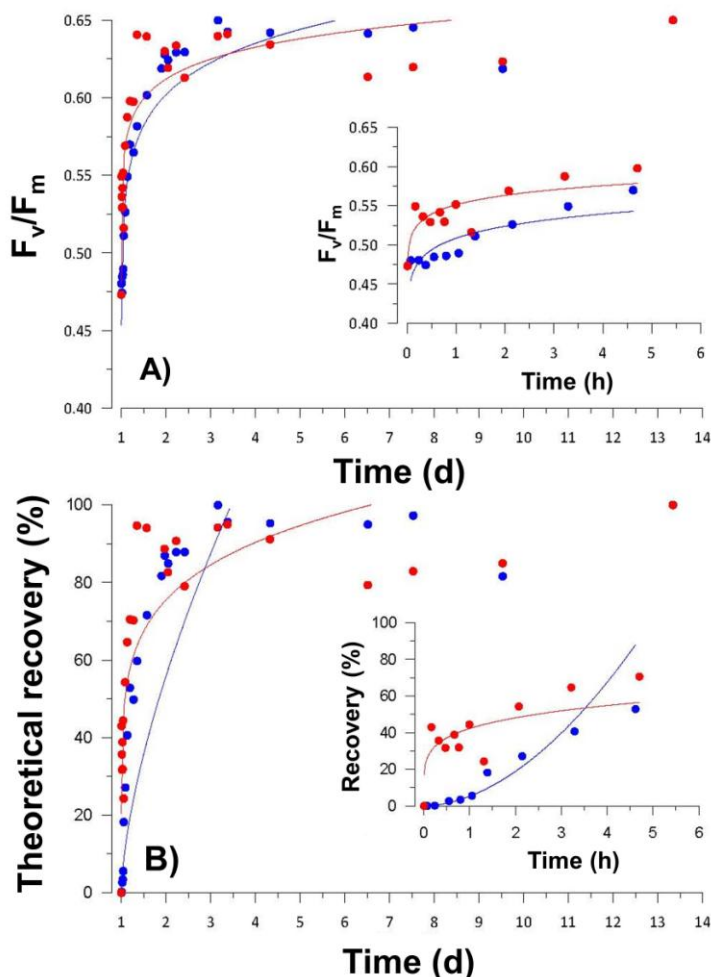


Figure 1. A) Long-term changes (over 13 days) of the potential photochemical efficiency of PSII for *P. antarctica* dominated natural assemblage (red circles) and *Pseudo-nitzschia* (blue circles) when incubated at a constant 300 μmol photons $\text{m}^{-2} \text{s}^{-1}$, and B) the percentage recovery of F_v/F_m over the same period. Inserts in each show the first 6 h of the response. Solid lines are a Ln:Ln regression.

PR 3 cultures were incubated in an on-deck incubator, and hence were exposed to natural solar radiation (including short-term fluctuations and diel changes) and greater average irradiance (the mean irradiance exposure over 24 hours was $\sim 450 \mu\text{mol}$ photons $\text{m}^{-2} \text{s}^{-1}$) than those in PR 2. The initial quantum yields for *P. antarctica* and *Pseudonitzschia* were 0.28 and 0.26, respectively, representing a significantly depressed photophysiological state (Figure 2). As with lower photoinhibitory irradiances, *P. antarctica* recovered much faster, achieving about 48% recovery within the first hour, in contrast to only 10% recovery in *Pseudonitzschia* (Table 2). However, both

fully recovered after ca. 24 h, indicating that recovery from short-term (daily) photoinhibitory recovery is rapid. In PR 4, an experiment designed to measure the short-term recovery kinetics, the initial F_v/F_m for *P. antarctica* and *Pseudo-nitzschia* were 0.23 and 0.29, respectively. *P. antarctica* once again recovered faster, achieving 55% recovery in the first hour vs. only 25 % in *Pseudonitzschia* (Figure. 3). Both species reached their relative maximum photosynthetic yields in ca. 8 h, faster than in the previous experiment. Two similar experiments (PR 7 and PR 8) produced similar results. Despite the minor variations in the rate of recovery among experiments, it is clear that *P. antarctica* had substantially more rapid recovery rates than did the diatom *Pseudonitzschia* sp.

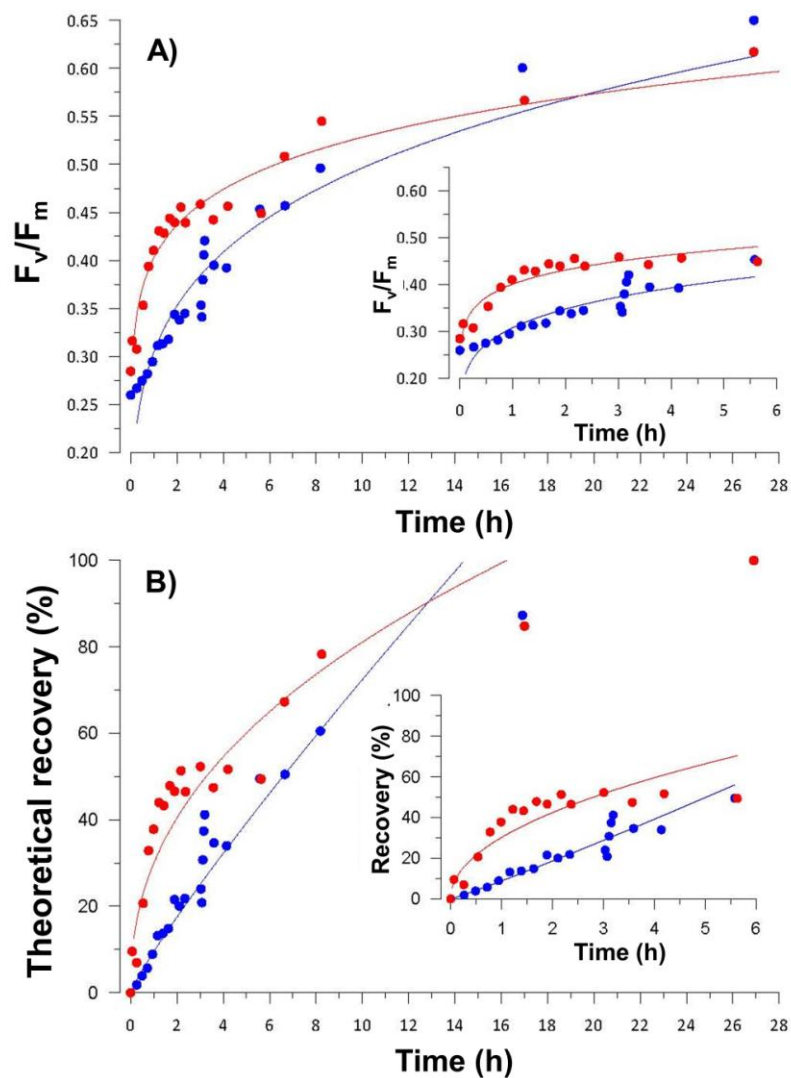


Figure 2. Short-term changes (27 h) of the potential photochemical efficiency of PSII for *P. antarctica* dominated natural assemblage (red circles) and *Pseudo-nitzschia* (blue circles) when incubated under in situ irradiance, and B) the percentage recovery of F_v/F_m through time. Insets in each show the first 6 h of the response. Solid lines are a Ln:Ln regression.

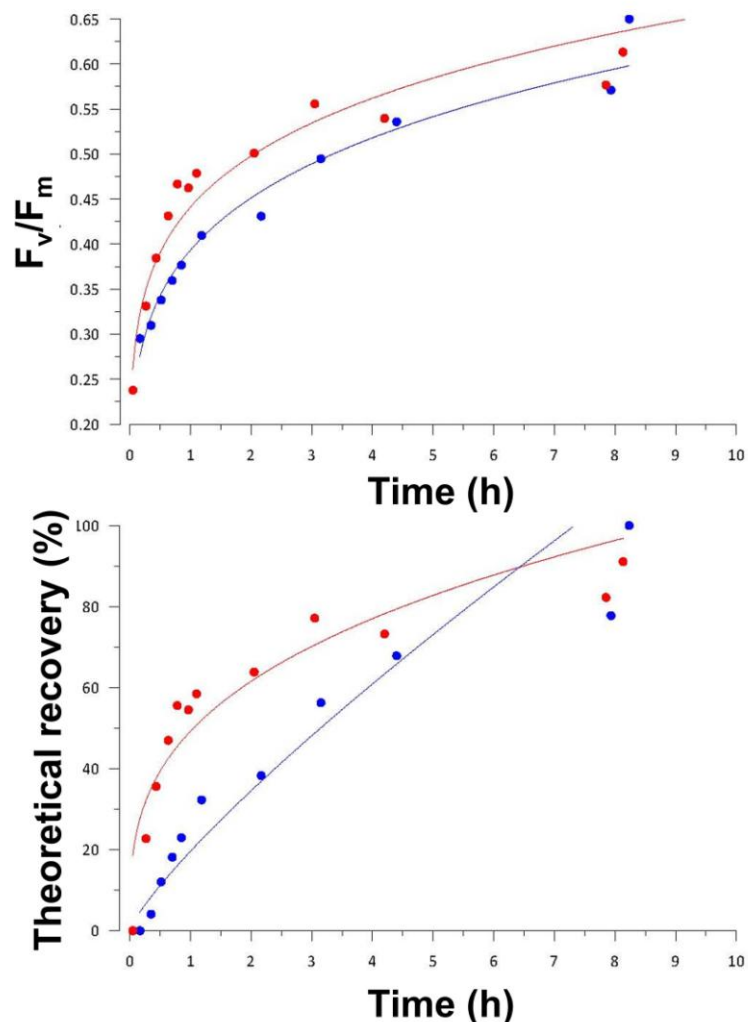


Figure 3. Short-term changes (~8 hours) of the potential photochemical efficiency of PSII for *P. antarctica* dominated natural assemblage (red circles) and *Pseudo-nitzschia* (blue circles) when incubated under in situ irradiance, and B) the percentage recovery of F_v/F_m through time. Solid lines are a Ln:Ln regression.

In PR 5 the two cultures underwent short exposures (2, 4, 6 and 8 h) to $\sim 850 \mu\text{mol photons m}^{-2} \text{ s}^{-1}$ to assess the impact of the length of time that inhibitory exposures in photorecovery rates (Figure. 4). Initial and final quantum yields in *P. antarctica* ranged from 0.37 (after 2 h exposure) to 0.25 after 8 h exposure, while those for *Pseudonitzschia* were 0.24 to 0.31. The duration of inhibitory exposure time was more important for *P. antarctica*, in that the extent of

photoinhibition was greater for longer exposures. In contrast, exposure duration had little impact on *Pseudo-nitzschia*. There was again a significant difference in the recovery time between species, with *P. antarctica* recovering faster than *Pseudonitzschia* (Figure 4). During the first photorecovery experiment of the spring cruise (PR 6), a 3-h exposure to 300 $\mu\text{mol photons m}^{-2} \text{ s}^{-1}$ induced limited photoinhibition in both cultures (Figure 5). Following the exposure *P. antarctica* quantum yields were 0.47, recovering to 0.52 after about five h and to 0.55 after ca. 24 h. *Pseudo-nitzschia* displayed an initial decrease in F_v/F_m to 0.45 and increased to 0.47 after 24 h (Figure 5).

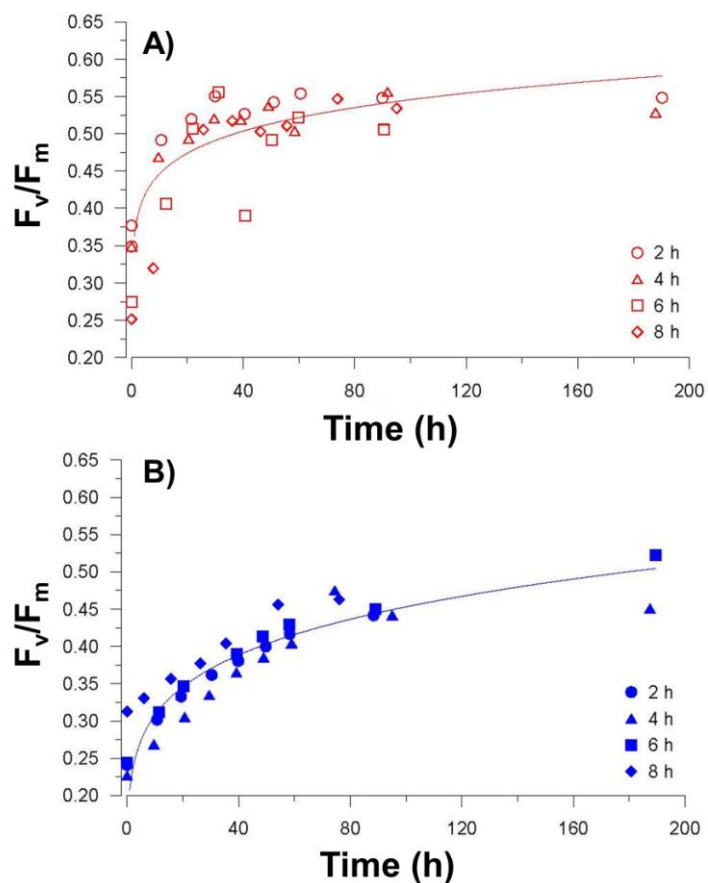


Figure 4. Changes over 8 days of the potential photochemical efficiency of PSII for A) *P. antarctica* dominated natural assemblage and B) *Pseudo-nitzschia* when incubated at a constant 850 $\mu\text{mol photons m}^{-2} \text{ s}^{-1}$ for 2 * circles), 4 (triangles), 6 (squares) or 8 (diamonds) h. Solid lines are a Ln:Ln regression for pooled data.

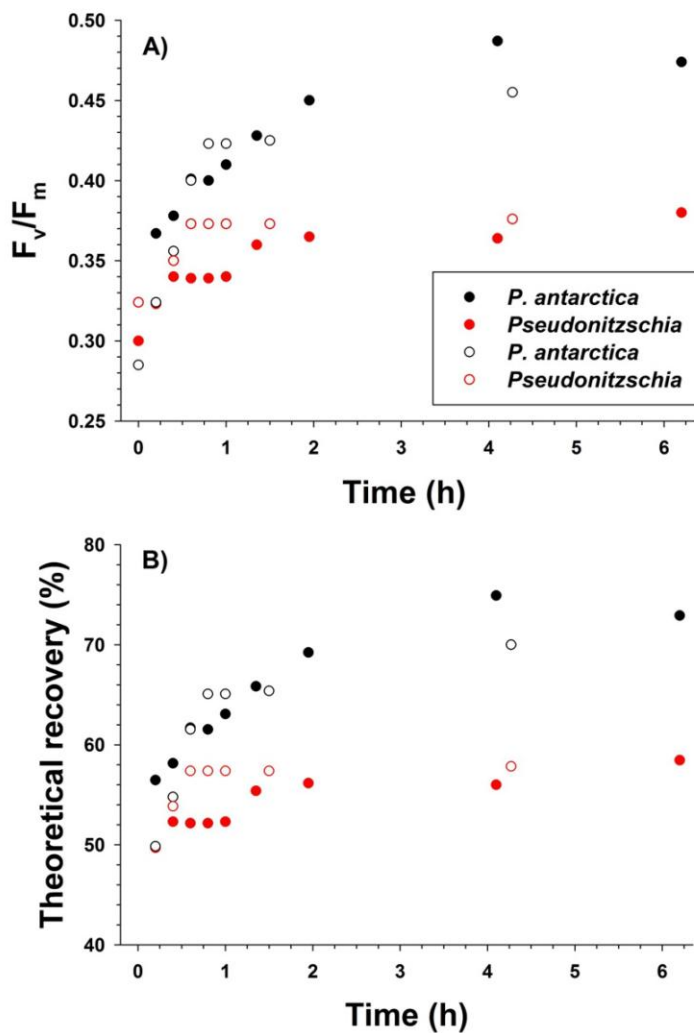


Figure 5. A) Short-term changes (8 hours) of the potential photochemical efficiency of PSII for *P. antarctica* and *Pseudo-nitzschia*; and B) theoretical percentage recovery of F_v/F_m over time. Filled symbols represent cultures exposed for 2 h to $600 \mu\text{mol photons m}^{-2} \text{ s}^{-1}$, and open symbols represent cultures exposed for 4 h at the same irradiance.

3.2. Trace Metal Addition Experiments

All three experiments added a series of trace elements (either singly or in dual additions), but only iron additions (or iron plus another trace component) generated a photophysiological response. In these experiments F_v/F_m of natural assemblages was initially 0.44 and steadily declined in all treatments and the control, except when iron was added (Figure. 6). Iron additions resulted in

increased or constant quantum yields, until after approximately five days when quantum yields began to decrease. The σ_{PSII} decreased upon iron addition, but increased in the experiments' later stages. A significant difference between iron treatments and all others was systematically observed for F_v/F_m and σ_{PSII} (LSM pair-wise comparison; Figure. 6). The low quantum yields found at the end of the experiments (ca. 0.28) are similar to those found in much of the Ross Sea during summer [20,25,26], suggesting that F_v/F_m values found in situ are reduced at least in part by strong iron limitation. Our results confirm that iron plays a major role in the photophysiological responses of Ross Sea phytoplankton.

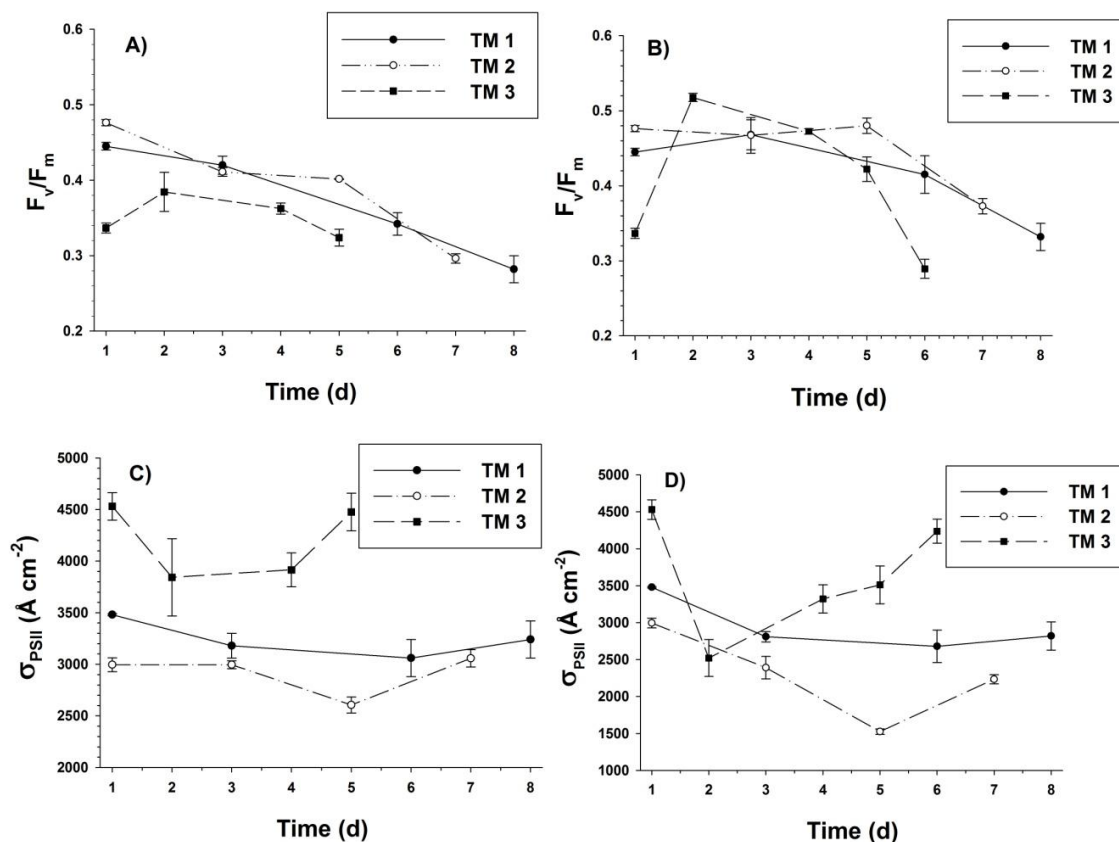


Figure 6. Time course of potential quantum yields and functional absorption cross sections of natural assemblages in response to iron additions. A) Potential quantum yield, no addition; B) Potential quantum yield, iron addition (1 nM); C) functional absorption cross section, no addition; and D) functional absorption cross section, iron addition.

4. Discussion

Phytoplankton experience large variations in irradiance over a variety of time scales, and need to acclimate to the environmental conditions that influence their growth. This is especially true in

waters of the Southern Ocean, where irradiance variations are as large as anywhere in the ocean. In addition to the substantial diel and seasonal variations, changes in mixed layer depths (which alter the vertical location of the population) also directly influence irradiance availability and the frequency of irradiance changes, and mixed layer depths respond rapidly (within hours) to changes in surface wind forcing [2]. The magnitudes of these variations can be large; for example, on three days in the southern Ross Sea mixed layers ranged from > 150 m to less than 20 m within one hour (Figure. 7). To understand the growth and strategies of phytoplankton in Antarctic waters, knowledge of the photophysiological responses to these extreme irradiance and environmental variations is needed. We designed experiments using the two major functional groups in the Ross Sea to begin to assess the rates of photorecovery to changes in irradiance, as well as the responses to trace metal concentrations (which also vary with mixed layer depths).

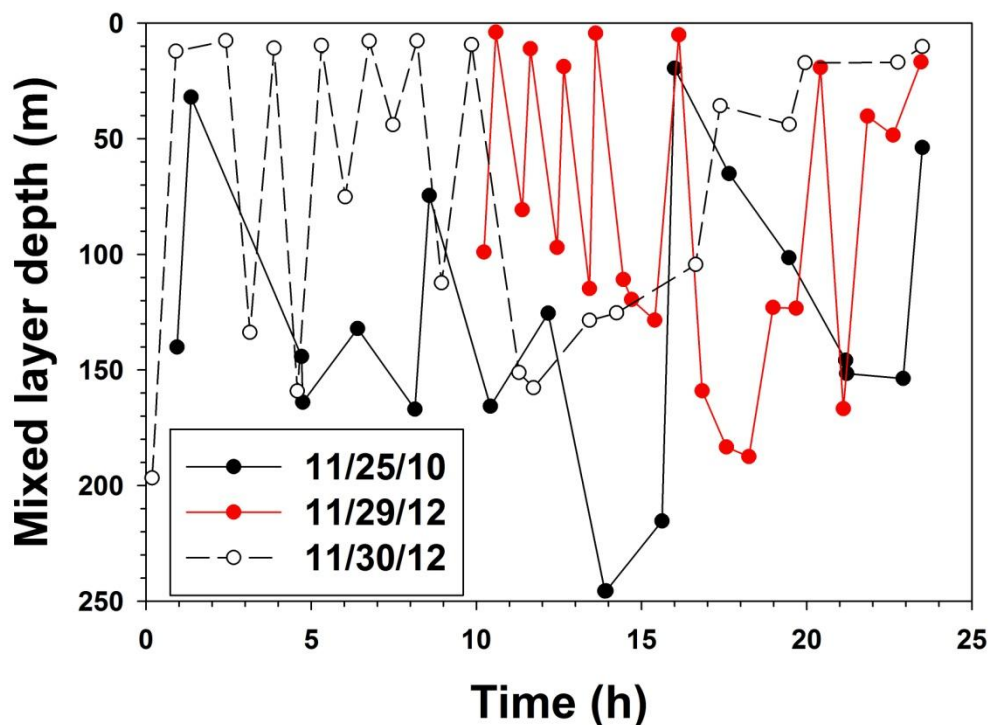


Figure 7. Changes in mixed layer depth over 24 h on three days in austral spring in the southern Ross Sea (~77.25°S, 169.5°E). Data available at: <http://www.bco-dmo.org/project/568868>.

High photon flux densities result in a depression of quantum yields. Smith et al. [20] found mean F_v/F_m values in spring to be 0.45 at the surface, but 0.57 at depth (80 m), a 21% reduction in quantum yield. Our experiments suggest that the photoinhibitory effects of high irradiances can be even greater on short time scales, but that recovery from photoinhibition is rapid enough to partially

remediate the depressed quantum yield. Smith et al. also reported that summer F_v/F_m values at the surface averaged 0.34 at the surface [20], but were the same as in spring at 80 m, suggesting that the effects of trace metals and irradiance largely disappear at depth, but that both play a significant role in generating reduced photosynthetic efficiency in the surface.

Populations of the haptophyte *Phaeocystis antarctica* recovered from inhibitory photon flux densities faster than did populations of a commonly found diatom, *Pseudonitzschia* sp., suggesting that it might be an adaptive response in rapidly changing environments and variable oceanographic conditions. Although there was some experimental variability in the recovery rates, *P. antarctica* always demonstrated nearly complete recovery within hours, whereas the diatom *Pseudonitzschia* recovered more slowly. Both, however, fully recovered by 24 h (Figures. 1-3). The total amount of inhibitory irradiance (that is, the length of time that a population was exposed to inhibitory fluxes) did not appear to influence the rate of recovery of the diatoms, whereas *P. antarctica* recovery tended to be more rapid for the lowest inhibitory fluxes (Figure. 4), suggesting that the absolute amount of energy absorbed by the haptophyte plays a larger role in photorecovery than in diatoms. *P. antarctica* has been shown to exhibit other photophysiological responses as well, such as modifying the production of photoprotective pigments. Moisan and Mitchell [27] showed that significant shifts at low irradiances from Chl *a*, 19-hexanoyloxyfucoxanthin and Chl *c* to diadinoxanthin, β -carotene, and diatoxanthin in *P. antarctica*, as well as fast xanthophyll cycling, which would provide an advantage in fluctuating light environments [28]. *P. antarctica* can also significantly increase its diatoxanthin/diadinoxanthin ratio in response to high irradiances [29]. Another photoacclimation mechanism observed in *P. antarctica* involves altering colonial size and cell concentration to compensate for the increased irradiance during spring, as well as producing mycosporine-like amino acids to withstand high irradiance levels [30]. *P. antarctica* also has a chlorophyll packaging ability [27], and can modify its quantum yield efficiency rapidly in response to short-term light variability. All of these potential mechanisms likely allow *Phaeocystis* to bloom in the Ross Sea during periods of exceptionally variable irradiance levels.

Not only can *P. antarctica* adjust to high irradiances under nutrient-replete conditions and maintain high photosynthetic capability over periods weeks (Figure. 1), it also has a remarkable ability of retaining photosynthetic competence through extended (month-long) exposures to darkness. Tang et al. [31] assessed quantum yields of cultures kept in the dark over a two-month period. During this time they observed an exponential decline of F_v/F_m ; nonetheless, at the end of the experiment the population was still photosynthetically viable and systematically recovered when re-exposed to light. This capacity undoubtedly enables *P. antarctica* populations to survive austral winter under complete darkness, beneath the vanishingly low irradiances encountered in spring under ice, and within the deep mixed layers characteristic of the Ross Sea in spring. October and November mixed layers can exceed 100 m (and in selected regions throughout the summer) [9], and *P. antarctica* is exposed to large time-dependent changes in irradiance in these regions. Hence the ability to recover rapidly from elevated irradiances, when combined with the ability to saturate

photosynthesis under low photon flux densities [19] and reduced losses due to grazing [32], provides the means for *P. antarctica* to grow and rapidly accumulate in the Ross Sea spring.

The trace metal addition experiments clearly indicated iron limitation of quantum yield (Figure 6). Conversely, there was no evidence that other trace elements (cobalt, vitamin B₁₂, zinc) had any impact on photosynthetic responses, despite the demonstration of potential co-limitation of phytoplankton growth by iron and vitamin B₁₂ [33]. A number of other investigations have also shown the strong and primary effect of iron [34–37], but few have assessed the suite of potential limiting factors on natural assemblages that we did in these experiments. Iron limitation of phytoplankton growth is commonly found in summer, but vitamin limitation has rarely been shown. Based on our results, we believe that the results of Bertrand [33] were likely driven by their sampling location and are not representative of the Ross Sea or Southern Ocean. Rose et al. and Feng et al. [35,36] experimentally manipulated irradiance, temperature, iron and CO₂ concentrations and measured quantum yield responses; both studies showed a modest (ca. 8%) increase under high iron concentrations in F_v/F_m ratios, but in both studies the effect was also modified by the other environmental variables. Kustka et al. [25] conducted long-term experiments (ca. 10 d) and found that additions of either ionic iron and siderophore-bound iron both significantly increased quantum yields, and Ryan-Keogh et al. [26] also demonstrated short-term (24 h) increases in F_v/F_m ratios upon iron addition. Our results provide further evidence of the important role of trace metals and specifically iron on phytoplankton photophysiology during summer in the Ross Sea.

5. Conclusions

Both haptophytes and diatoms can experience reduced quantum yields in response to elevated photon flux densities. Ross Sea phytoplankton taxa have significantly different photophysiological responses to irradiance, which are consistent with the strategy for one, *Phaeocystis antarctica*, to thrive in low irradiance environments with significant variability on various times scales. *Phaeocystis* recovers more rapidly than diatoms, but both recover from photoinhibitory photon flux densities within 24 h. Rapid recovery may be characteristic of energetic water columns with extensive vertical mixing. Enhanced F_v/F_m ratios are found at elevated iron concentrations but not with increased concentrations of cobalt, vitamin B₁₂, or zinc, confirming the importance of iron on photophysiological responses in the Ross Sea. The photophysiology of *Phaeocystis* is likely the primary reason for its regular growth and accumulation in the spring in the Ross Sea.

Acknowledgements

This research was funded by grants from the US NSF (OPP-0087401 and ANT-1443258). We thank all our CORSACS colleagues, especially M. Saito, P. Sedwick and Z. Kolber. This paper is Contribution No. 3633 of the Virginia Institute of Marine Science, College of William & Mary.

Conflict of interest

Both authors declare no conflicts of interest in this paper.

References

1. Kirk JTO (1994) *Light and photosynthesis in aquatic ecosystems*. Cambridge University Press, Cambridge, UK.
2. Jones RM and Smith WO Jr (2017) The influence of short-term events on the hydrographic and biological structure of the southwestern Ross Sea. *J Mar Systems* 166: 184-195.
3. Smith WO Jr and Nelson DM (1985) Phytoplankton bloom produced by a receding ice edge in the Ross Sea: spatial coherence with the density field. *Sci* 227: 163-166.
4. Arrigo KR and McClain CR (1994) Spring phytoplankton production in the western Ross Sea. *Sci* 266: 261-263.
5. Arrigo KR, Robinson DH, Worthen DL, et al. (1999) Phytoplankton community structure and the drawdown of nutrients and CO₂ in the Southern Ocean. *Sci* 283: 365-367.
6. Smith WO Jr and Gordon LI (1997) Hyperproductivity of the Ross Sea (Antarctica) polynya during austral spring. *Geophys Res Letters* 24: 233-236.
7. Rousseau V, Chrétiennot-Dinet M-J, Jacobsen A, et al. (2007) The life cycle of *Phaeocystis*: state of knowledge and presumptive role in ecology. *Biogeochem* 83: 29-47.
8. Smith WO Jr, Ainley DG, Arrigo KR, et al (2014) The oceanography and ecology of the Ross Sea. *Annu Rev Mar Sci* 6: 469-487.
9. Smith WO Jr and Jones RM (2015) Vertical mixing, critical depths, and phytoplankton growth in the Ross Sea. *ICES J. Mar. Sci* 72: 1952-1960.
10. Leventer A and Dunbar RB (1996) Factors influencing the distribution of diatoms and other algae in the Ross Sea. *J Geophys Res* 101: 18489-18500.
11. Nuccio C, Innamorati M, Lazzara L, et al. (2000) Spatial and temporal distribution of phytoplankton coenoses in the Ross Sea. In: Faranda FM, Guglielmo L, Ianora A (Eds.), *Ross Sea Ecology. Italianantartide Expeditions (1987-1995)*. Springer Verlag, Berlin, 231-245.
12. Fonda Umani S, Accornero A, Budillon G, et al (2002) Particulate matter and plankton dynamics in the Ross Sea Polynya of Terra Nova Bay during the austral summer 1997/98. *J Mar Syst* 36: 29-49.
13. McGillicuddy DM Jr, Sedwick PN, Dinniman MS, et al. (2015) Iron supply and demand in an Antarctic shelf system. *Geophys Res Letters* 42:.
14. Falkowski PG and Raven JA (1997) *Aquatic Photosynthesis*. Princeton Univ Press, Princeton, NJ.
15. Kropuenske LR, Mills MM, van Dijken GL, et al. (2009) Photophysiology in two major Southern Ocean phytoplankton taxa: Photoprotection in *Phaeocystis antarctica* and *Fragilariaopsis cylindrus*. *Limnol Oceanogr* 54: 1176-1196.

16. Vass I, Styring S, Hundal T, et al (1992) Reversible and irreversible intermediates during photoinhibition of photosystem II: stable reduced QA species promote chlorophyll triplet formation. *Proc Nat Acad Sci US* 89: 1408-1412.
17. Demmig-Adams B and Adams WW (1992) Photoprotection and other responses of plants to high light stress. *Annu Rev Plant Physiol Plant Mol Biol* 43: 599-626.
18. Smith WO Jr and Donaldson K (2015) Photosynthesis-irradiance responses in the Ross Sea, Antarctica: a meta-analysis. *Biogeosci* 12: 1-11.
19. Arrigo KR, Mills MM, Kropuenske LR, et al (2010) Photophysiology in two major southern ocean phytoplankton taxa: photosynthesis and growth of *Phaeocystis antarctica* and *Fragilariaopsis cylindrus* under different irradiance levels. *Integr Compar Biol* 50: 950-966.
20. Smith WO Jr, Tozzi S, Sedwick PW, et al. (2013) Spatial and temporal variations in variable fluorescence in the Ross Sea (Antarctica): environmental and biological correlates. *Deep-Sea Res I* 79: 141-155.
21. Genty B, Briantais JM, Baker NR (1989) The relationship between the quantum yield of photosynthetic electron transport and quenching of chlorophyll fluorescence. *Biochim Biophys Acta* 990: 87-92.
22. Kolber ZS, Prasil O, Falkowski PG (1998) Measurements of variable chlorophyll fluorescence using fast repetition rate techniques: defining methodology and experimental protocols. *Biochim Biophys Acta* 1367: 88-106.
23. Keller MD, Selvin RC, Claus W, et al. (1987) Medifor the culture of oceanic ultraphytoplankton. *J Phycol* 23: 633-638.
24. Sedwick PN, Marsay CM, Aguilar-Islas AM, et al. (2011) Early-season depletion of dissolved iron in the Ross Sea polynya: implications for iron dynamics on the Antarctic continental shelf. *J Geophys Res* 116.
25. Kustka AB, Jones BM, Hatta M, et al. (2015) The influence of iron and siderophores on eukaryotic phytoplankton growth rates and community composition in the Ross Sea. *Mar Chem* 173: 195-207.
26. Ryan-Keogh TJ, Delizo LM, Smith WO Jr, et al. (2016) Temporal progression of photosynthetic strategy by phytoplankton in the Ross Sea, Antarctica. *J Mar Systems* 166: 87-96.
27. Moisan TA, Mitchell BG (1999) Photophysiological acclimation of *Phaeocystis antarctica* Karsten under light limitation. *Limnol Oceanogr* 44: 247-258.
28. Moisan TA, Olazola M, Mitchell BG (1998) Xanthophyll cycling in *Phaeocystis antarctica*: changes in cellular fluorescence. *Mar Ecol Prog Ser* 169: 113-121.
29. Van Leeuwe MA and Stefels J (1998) Effects of iron and light stress on the biochemical composition of Antarctic *Phaeocystis* sp.(Prymnesiophyceae). II. Pigment composition. *J Phycol* 34: 496-503.
30. Liselotte R and Dale R. (1997) Photoinduction of UV-absorbing compounds in Antarctic diatoms and *Phaeocystis antarctica*. *Mar Ecol Prog Ser* 160: 13-25.

31. Tang KW, Smith WO Jr, Shields AR, et al. (2009) Survival and recovery of *Phaeocystis antarctica* (Prymnesiophyceae) from prolonged darkness and freezing. *Phil Trans Roy Soc, ser B* 276: 81-90.
32. Caron DA, Dennett MR, Lonsdale DJ, et al. (2000) Micro-zooplankton herbivory in the Ross Sea, Antarctica. *Deep Sea Res II* 47: 3249-3272.
33. Bertrand EM, Saito MA, Rose JM, et al. (2007) Vitamin B₁₂ and iron co-limitation of phytoplankton growth in the Ross Sea. *Limnol Oceanogr* 52: 1079-1093.
34. Sedick PN and DiTullio GR (1997) Regulation of algal blooms in Antarctic shelf waters by the release of iron from melting sea ice. *Geophys Res Letters* 24: 2515-2518.
35. Feng Y, Hare CE, Rose JM, et al. (2010) Interactive effects of CO₂, irradiance and iron on Ross Sea phytoplankton. *Deep Sea Res I* 57: 368-383.
36. Rose JM, Feng Y, DiTullio G, et al. (2009) Synergistic effects of iron and temperature on Antarctic plankton assemblages. *Biogeosci* 6: 3131-3147.
37. Xu K, Fu F-X, Hutchins DA (2014) Comparative responses of two dominant Antarctic phytoplankton taxa to interactions between ocean acidification, warming, irradiance, and iron availability. *Limnol Oceanogr* 59: 1919-1931.



AIMS Press

© 2017 Walker O. Smith, et al., licensee AIMS Press. This is an open access article distributed under the terms of the Creative Commons Attribution License (<http://creativecommons.org/licenses/by/4.0>)